J Mater Sci (2008) 43:3946–3953
DOI 10.1007/s10853-007-2373-4

Effect of coherency on coarsening of second-phase precipitates in Cu-base alloys

Daizen Watanabe · Chihiro Watanabe · Ryoichi Monzen

Received: 7 July 2007 / Accepted: 3 December 2007 / Published online: 21 March 2008

Abstract The effects of matrix/precipitate interface states on coarsening of Co and γ-Fe precipitates in a Cu–4 wt.%Co and a Cu–2 wt.%Fe alloy aged at 500 and 700 °C have been examined by transmission electron microscopy (TEM) observations, electrical resistivity measurements, and length-change measurements. Analyses of TEM images show that the average radius for coherent/semi-coherent transition is 6–12 nm for the Co precipitates and 10–20 nm for the γ-Fe precipitates. The coarsening rates of the Co and γ-Fe precipitates are unchanged by the transitions in coherency of the precipitates. The interface energies γ of coherent Co and γ-Fe precipitates are estimated from data on coarsening alone as 0.15 and 0.27 J m^{-2}. From length-change measurements of the Cu–Co and Cu–Fe alloys during aging, the estimates of the isotropic misfit strains of Co and γ-Fe precipitates are -0.018 and -0.016 for the coherent interfaces and -0.013 and -0.012 for the semi-coherent interfaces. Free energy analyses for the coarsening of Co and γ-Fe precipitates reveal that the values of γ of semi-coherent Cu/Co and Cu/γ-Fe interfaces are 0.24 and 0.34 J m^{-2}.

Introduction

In a previous paper [1], we have studied the coarsening of fcc Co precipitates in a Cu–1 wt.%Co alloy aged at 600–725 °C by transmission electron microscopy (TEM) observations and electrical resistivity measurements. The average radius of Co precipitates increases with aging time t as $t^{1/3}$, as described by the theory of Lifshitz and Slyozov [2] and Wagner [3] (LSW). The kinetics of the depletion of Co supersaturation obeys the $t^{-1/3}$ time law, deduced from the LSW theory modified by Ardell [4]. The coarsening rate of Co precipitates was not affected by the change in coherency from a coherent interface to a semi-coherent interface, namely the introduction of misfit dislocations to the coherent interface. The Cu/Co interface energy γ and diffusion coefficient D of Co in the Cu matrix were derived independently from data on coarsening alone using the LSW theory. The value of $\gamma = 0.15$ J m^{-2} was obtained mainly for semi-coherent Co precipitates, i.e., we could not determine accurately a value of γ for the coherent interface, because of only one data point in a coherent stage on the coarsening curve at 700 °C.

When a Cu alloy with Fe less than about 3% is aged at an elevated temperature, spherical, coherent γ-Fe precipitates are first formed [5]. Monzen and Kita [6] have investigated the coarsening behavior of γ-Fe precipitates in Cu–1.0 wt.%Fe and Cu–1.7 wt.%Fe alloys on aging at 600–700 °C using combined techniques of TEM and electrical resistivity measurements. The coarsening of γ-Fe precipitates follows the LSW theory and the Fe concentration in the matrix during coarsening decreases with t as $t^{-1/3}$. The value of γ for the Cu/γ-Fe interface was independently evaluated as about 0.25 J m^{-2} using the LSW theory without a value of D. However, the effect of the interfacial state on γ was not studied.

In this study, we investigate the effects of coherency on the coarsening of Co and γ-Fe precipitates in a Cu–4 wt.%Co and a Cu–2 wt.%Fe alloy aged at 500 and 700 °C in detail. The coherent interface energies of Co and γ-Fe precipitates have been accurately estimated. The transitions from the coherent Cu/Co and Cu/γ-Fe

D. Watanabe · C. Watanabe · R. Monzen (✉)
Division of Innovative Technology and Science, Kanazawa University, Kakuma-machi, Kanazawa 920-1192, Japan
e-mail: monzen@t.kanazawa-u.ac.jp

interfaces to the semi-coherent interfaces have not affected the interface energies of the precipitates experimentally determined using the LSW theory, similar to the result of the previous study [1]. This result is uncertain, since it is widely accepted that the introduction of misfit dislocations to a coherent interface causes an increase in the coherent interface energy [7–10]. This point will be discussed by examining the driving force for coarsening of the coherent and semi-coherent precipitates. The driving force for coarsening is dependent on the elastic strain energy of a precipitate [11]. Length-change measurements have thus been undertaken to estimate the misfit strains of Co and γ-Fe precipitates in coherent and semi-coherent states.

Experimental

Ingots of Cu–4 wt.%Co and Cu–2 wt.%Fe alloys were prepared by melting 99.99 wt.%Cu, a Cu–10.5 wt.%Co master alloy and a Cu–10.0 wt.%Fe master alloy. The alloy ingots were homogenized at 900 °C for 24 h in a vacuum. Specimen pieces were cut from the ingots and cold-rolled to a thickness of 3 mm. Then the specimens were solution-treated at 1050 °C for 5 h in a vacuum, quenched into cold water, and subsequently aged at 500 and 700 °C in a vacuum.

Thin foils, 0.2 mm thick, for TEM observations were prepared from the aged specimens by electropolishing using a solution of 20 vol.% phosphoric acid. Microscopy was performed using a JEOL 2010FEF or a HITACHI H-9000NAR microscope at an operation voltage of 200 or 300 kV. The precipitate coherency was examined using the Ashby–Brown contrast [12, 13] around precipitates in bright-field images. The detailed procedure of coherency judgments is described in the literature [7].

The solution-treated specimens for electrical resistivity measurements were spark-cut to the size of 100 mm × 10 mm × 0.5 mm. After aging, resistivity measurements were made at 20 °C using a standard four-point potentiometric technique. The cross-sectional area of the specimen was measured at different positions and the average value was used. By applying the experimental data obtained by Linde [14], the Co and Fe concentrations in the Cu matrix were determined.

Length changes on aging were examined by measuring, with a micrometer, the distance between two scratched marks of 20 mm × 5 mm × 3 mm-sized specimen. The length between the two marks of solution-treated specimens is about 10 mm. An X-ray analysis was performed to examine the lattice constants of the solution-treated and aged specimens. A diffractometer with a Cu target was used.

Results

Coarsening kinetics of Co and γ-Fe precipitates

Figures 1 and 2 show bright-field images of γ-Fe precipitates in a Cu–2 wt.%Fe alloy aged at 700 °C, taken using the matrix $[001]_{Cu}$ and $[011]_{Cu}$ zone axes, respectively. It is apparent from Figs. 1(a) and 2(a) that the shape of small γ-Fe precipitates is spherical. When the γ-Fe precipitates become larger than about 25 nm in radius, they changed into a nearly cuboidal shape faceted on $\{001\}_{Cu}$ planes. Examples of cuboidal precipitates are shown in Figs. 1(b) and 2(b). Even after the shape change occurred, the cube-on-cube orientation relationship was satisfied between the γ-Fe precipitates and the matrix. On the other hand, the shape of Co precipitates in the Cu matrix changed from a sphere to a octahedron with flat interfaces parallel to $\{111\}_{Cu}$ planes via a cube faceted on $\{001\}_{Cu}$ planes, in agreement with our previous result for a Cu–1 wt.%Co alloy aged at 600–725 °C [1]. The transitions from the

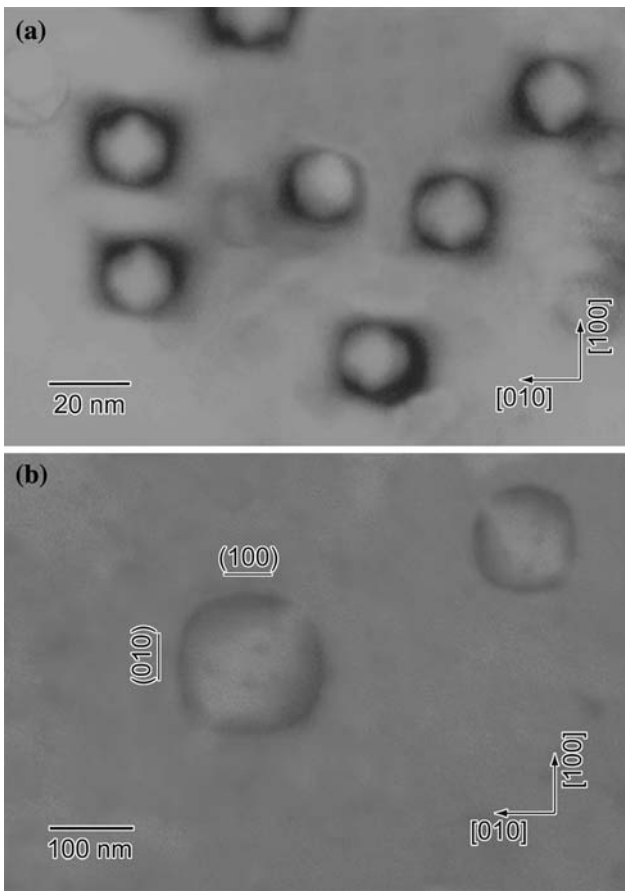

Fig. 1 Bright-field images of γ-Fe precipitates in a Cu–2 wt.%Fe alloy aged at 700 °C for (**a**) 30 min and (**b**) 100 h. The zone axis is $[001]_{Cu}$

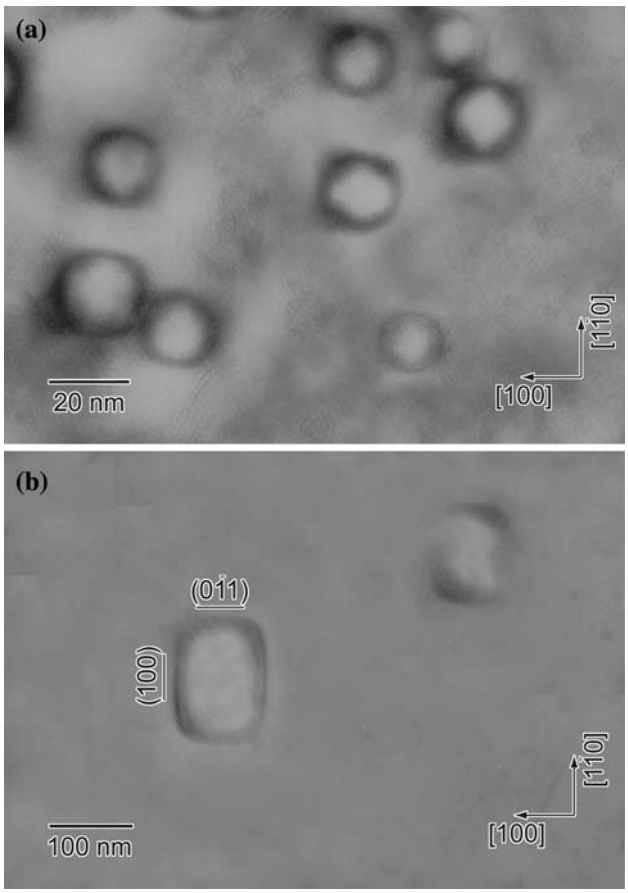

Fig. 2 Bright-field images of γ-Fe precipitates in a Cu–2 wt.%Fe alloy aged at 700 °C for (**a**) 30 min and (**b**) 100 h. The zone axis is $[011]_{Cu}$

sphere to the cube and from the cube to the octahedron occur at the radius of about 14 and 35 nm, respectively [1].

Figure 3 presents the ratio R of semi-coherent Co and γ-Fe precipitates to the total number of the Co and γ-Fe precipitates at each average radius r. Similar to our previous observation for the Cu–1 wt.%Co alloy [1], there exist three stages in the precipitation processes of Co and γ-Fe precipitates: a coherent stage where almost all precipitates are coherent with the matrix, a mixed stage at which coherent and semi-coherent precipitates coexist, and a semi-coherent stage, with almost all precipitates being semi-coherent with the matrix. The semi-coherent Co precipitates rapidly increase from 6 to 12 nm and the semi-coherent γ-Fe precipitates from 10 to 20 nm. The average radii of $r_c = 6$ and 10 nm for the transition of coherency of Co and γ-Fe precipitates are almost identical to the values of 6.8 and 8.7 nm calculated from $r_c = b/2\delta$, where b is the magnitude of Burgers vector, 0.2509 nm for Co [15] and 0.2519 nm for γ-Fe [16], and δ is the lattice misfit between Cu and Co or γ-Fe. The values of $\delta = -0.019$ and -0.015 for the Co and γ-Fe precipitates calculated using the lattice constants of $a = 0.3548$ nm for fcc Co [15], $a = 0.3562$ nm for γ-Fe [16], and $a = 0.3615$ nm for Cu [17] were employed. The high-resolution TEM observations often showed the existence of misfit dislocations at the interfaces of the Co and γ-Fe precipitates larger than about 6 and 10 nm, respectively.

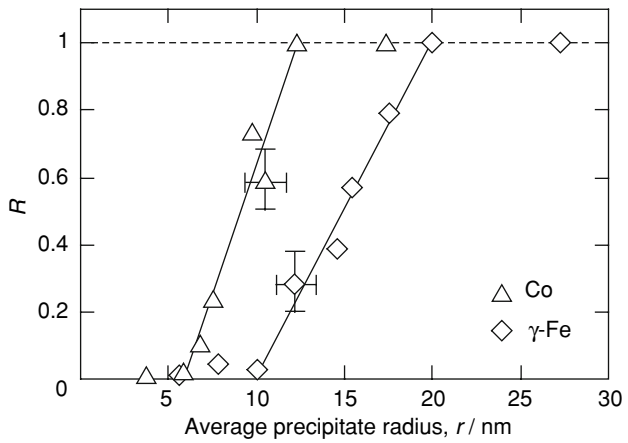

Fig. 3 Variation in the ratios R of semi-coherent Co and γ-Fe precipitates to the total number of precipitates with average radius r

As mentioned above, large Co and γ-Fe precipitates had non-spherical shapes. The radius of a sphere with volume identical to that of a non-spherical precipitate was calculated. The coarsening data thus obtained are presented in Fig. 4, where r is plotted against t on logarithmic scales. Lines with slope of 1/3, representing the prediction of the LSW theory, are superimposed. The shaded and hatched areas indicate the mixed stages of the precipitation processes. The data points deviate slightly from the lines at initial times, but approach the lines as t increases. It is

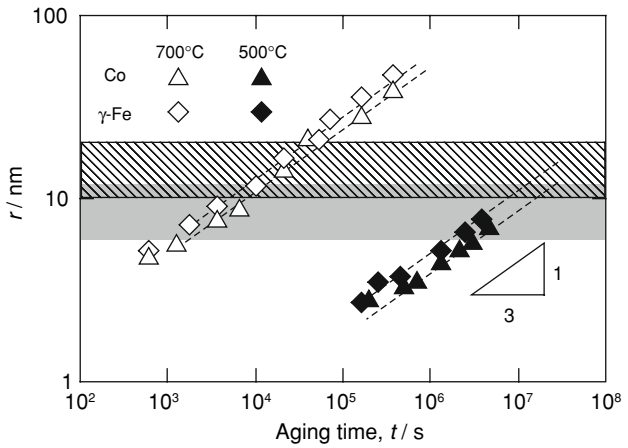

Fig. 4 Variation in the average precipitate radius r with aging time t for a Cu–4 wt.%Co and a Cu–2 wt.%Fe alloy aged at 500 and 700 °C. Lines with slope of 1/3 are superimposed. The shaded and hatched areas indicate the mixed stages for Co precipitates ($6 < r < 12$ nm) and γ-Fe precipitates ($10 < r < 20$ nm), respectively

evident that the growth kinetics of Co and γ-Fe precipitates are unaffected by the transition in precipitate coherency.

According to the LSW theory, the cube of the average precipitate radius r^3 increases with time t as follows:

$$r^3 - r_0^3 = K(t - t_0), \tag{1}$$

$$K = \frac{8D\gamma C_e V_m^2}{9RT}, \tag{2}$$

where r_0 is the average radius at the onset of coarsening at time t_0, K is a rate constant, D is the diffusivity of the solute atom in Cu, γ is the energy of the matrix/precipitate interface, C_e is the equilibrium concentration of solute in the matrix, V_m is the molar volume of the precipitate, and RT has its usual meaning. The values of V_m of the fcc Co and γ-Fe precipitates are calculated to be 6.72×10^{-6} m^3 mol^{-1} and 6.80×10^{-6} m^3 mol^{-1} from $V_m = a^3 N_a/4$, where N_a is the Avogadro's number.

Figures 5 and 6 show the coarsening plots of the Co and γ-Fe precipitates in Cu–4 wt.%Co and Cu–2 wt.%Fe alloys aged at 500 and 700 °C, respectively. The shaded and hatched areas indicate the mixed stages. In Fig. 5, the growth rates on aging at 500 °C decrease gradually in the initial stage of aging as indicated by dashed lines and then reach constant values after certain times. In contrast, the growth rates at 700 °C are nearly constant from the beginning, as seen in Fig. 6. The starting time of the r^3 growth law for the Co and γ-Fe precipitates are 150 and 120 h (5.4×10^5 and 4.3×10^5 s) on aging at 500 °C and 20 and 30 min (1.2×10^3 and 1.8×10^3 s) on aging at 700 °C. Since the constant growth rates of the Co and γ-Fe precipitates are attained in the coherent stages, the changes in growth rate cannot be attributed to the transitions in coherency. The slopes of the straight lines, determined by the least-squares method, give experimental values of K.

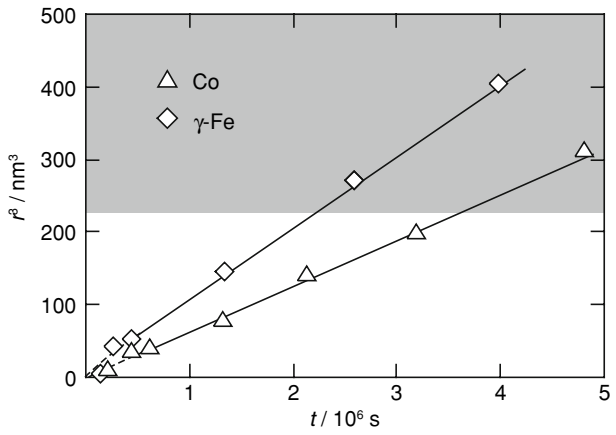

Fig. 5 Coarsening plots of Co and γ-Fe precipitates in Cu–4 wt.%Co and Cu–2 wt.%Fe alloys aged at 500 °C. The shaded area indicates the mixed stage where coherent and semi-coherent Co precipitates coexist

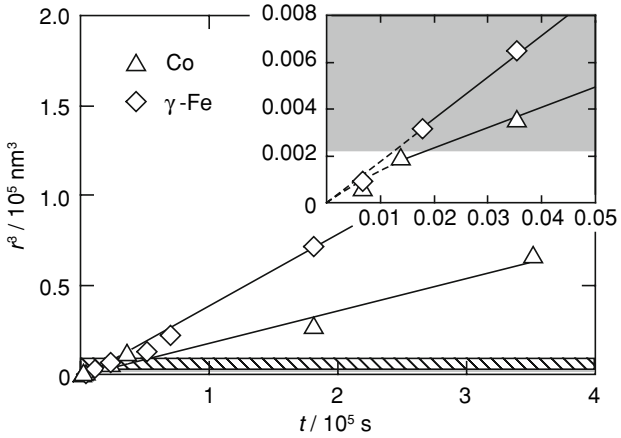

Fig. 6 Coarsening plots of Co and γ-Fe precipitates in Cu–4 wt.%Co and Cu–2 wt.%Fe alloys aged at 700 °C. The shaded and hatched areas indicate the mixed stages for Co precipitates and γ-Fe precipitates, respectively

Table 1 lists the values of K. The value of K at 700 °C for γ-Fe is nearly identical to $K = 3.79 \times 10^{-28}$ m^3 s^{-1} for the γ-Fe precipitates in a Cu–1.7 wt.%Fe alloy aged at 700 °C [6], but the value of K at 700 °C for Co is larger than $K = 6.50 \times 10^{-29}$ m^3 s^{-1} for the Co precipitates in a Cu–1.0 wt.%Co alloy aged at 700 °C [1]. The increase in K with increasing Co concentration is a consequence of the dependence of the coarsening constant on the finite volume fraction of Co precipitates present during coarsening. Hereafter, the effect of the volume fraction on K will not be discussed, since this problem is beyond the scope of this study.

The LSW theory of coarsening predicts that the solute concentration C in the matrix during coarsening varies with time t as

$$C - C_e = (kt)^{-1/3}, \tag{3}$$

where k is a coarsening parameter given by Ardell [4] and is expressed as

$$k = \frac{D}{9V_m}\left(\frac{RT}{\gamma C_e}\right)^2. \tag{4}$$

Following Eq. 3, plots of C against $t^{-1/3}$ are depicted in Fig. 7. The solute concentration C exhibits a rapid decrease at the initial stage of aging as illustrated by a dashed line, and a linearity is observed between C and $t^{-1/3}$, after times of $t = 150$ h and 20 min ($t^{-1/3} = 0.0123$ and 0.0941 s$^{-1/3}$) for the Cu–4 wt.%Co alloy aged at 500 and 700 °C, and of $t = 120$ h and 30 min ($t^{-1/3} = 0.0132$ and 0.0822 s$^{-1/3}$) for the Cu–2 wt.%Fe alloy aged at the same temperatures. These onset times of the $t^{-1/3}$ time law are identical to those of the r^3 growth law in Figs. 5 and 6. Thus the coarsening begins at these times. The changes in growth rates of the Co and γ-Fe precipitates in Figs. 5 and 6 may

Table 1 Values of the rate constant K and coarsening parameter $k^{-1/3}$ for Cu–4 wt.%Co and Cu–2 wt.%Fe alloys

T (°C)	K (m^3 s^{-1})		$k^{-1/3}$(mol m^{-3} $s^{1/3}$)	
	Co	γ-Fe	Cu–4Co	Cu–2Fe
500	$(7.00 \pm 0.10) \times 10^{-32}$	$(1.04 \pm 0.02) \times 10^{-31}$	1600 ± 155	1700 ± 145
700	$(1.77 \pm 0.19) \times 10^{-28}$	$(4.10 \pm 0.14) \times 10^{-28}$	423 ± 50	350 ± 45

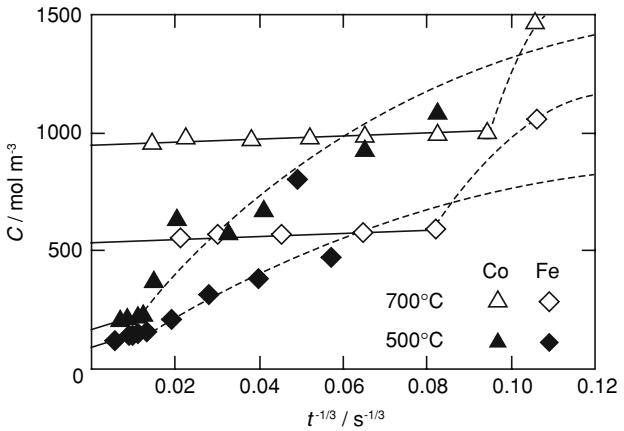

Fig. 7 Variation in the solute concentrations C in the matrix of Cu–4 wt.%Co and Cu–2 wt.%Fe alloys aged at 500 and 700 °C as a function of $t^{-1/3}$

be caused by the transitions from blended stages of growth and coarsening to coarsening stages, as in the previous study [1]. From the slopes and the intercepts of the solid lines in Fig. 7, values of $k^{-1/3}$ and C_e were estimated. Tables 1 and 2 list the values of $k^{-1/3}$ and C_e, together with the C_e values at 700 °C previously reported [1, 6]. The derived values of C_e are in agreement with the reported values.

Combination of Eqs. 2 and 4 enables the interface energy γ to be calculated without assuming a value for D. For this calculation, it is unnecessary to correct for the volume fraction of Co precipitates, since the appropriate factors depending on the volume fraction cancel. The resulting values are shown in Table 3, together with the values of γ for Co and γ-Fe previously reported [1, 6]. The estimates of γ for Co and γ-Fe are, on average, 0.15 and 0.27 J m^{-2}, respectively. The former and latter values are in good agreement with our previous value of 0.15 J m^{-2} [1] and the value of about 0.25 J m^{-2} previously reported by Monzen and Kita [6] and other researchers [18–21].

Misfit strains of Co and γ-Fe precipitates

Initially, the misfit strains ε_{ij}^{P} of spherical Co and γ-Fe precipitates for both the coherent and semi-coherent interfaces are assumed to have components of $\varepsilon_{ij}^{P} = \delta_{ij}\varepsilon$, where δ_{ij} is the Kronecker delta. When ε^{T} is the isotropic stress-free transformation strain of the equivalent inclusion which has the same elastic constants as the matrix and produces the elastic state, identical to that due to the actual precipitate [22], then the elongation ε_t of an elastically isotropic specimen is written as [23]

$$\varepsilon_t = f\varepsilon^{T} + (1-f)\varepsilon^{a}. \quad (5)$$

Here f is the volume fraction of the precipitates and ε^{a} is the dimensional change due to the loss of Co or Fe solute atoms from the supersaturated matrix.

Figure 8 presents the elongations ε_t of Cu–4 wt.%Co and Cu–2 wt.%Fe specimens aged at 700 °C as a function of aging time t. ε_t exhibits initially a rapid decrease, then a plateau behavior between 20 min and 2 h (1.2×10^3 and 7.2×10^3 s) for Cu–Co and between 30 min and 3 h (1.8×10^3 and 1.1×10^4 s) for Cu–Fe, a subsequent increase, and finally a plateau behavior after 6 h (2.2×10^4 s) for Cu–Co and 15 h (5.4×10^4 s) for Cu–Fe. The times of 20 and 30 min for Cu–Co and Cu–Fe are in agreement with the onset times of coarsening of the

Table 2 Values of the equilibrium concentration C_e of Co and Fe in the Cu matrix, obtained from analysis of data on coarsening

T (°C)	C_e (wt.%)			
	Co		Fe	
	Present study	Watanabe et al.	Present study	Monzen and Kita
500	0.13 ± 0.01	–	0.084 ± 0.005	–
700	0.60 ± 0.01	0.60	0.33 ± 0.01	0.50

Also shown are values of C_e reported by Watanabe et al. [1] and Monzen and Kita [6]

Table 3 Values of the energy γ of Cu/Co and Cu/γ-Fe interface, obtained from analysis of data on coarsening of Co and γ-Fe precipitates

T (°C)	γ (J m^{-2})			
	Cu/Co interface		Cu/γ-Fe interface	
	Present study	Watanabe et al.	Present study	Monzen and Kita
500	0.15 ± 0.02	0.15	0.27 ± 0.02	0.24–0.27
700	0.15 ± 0.02		0.28 ± 0.03	

Also shown are values of γ reported by Watanabe et al. [1] and Monzen and Kita [6]

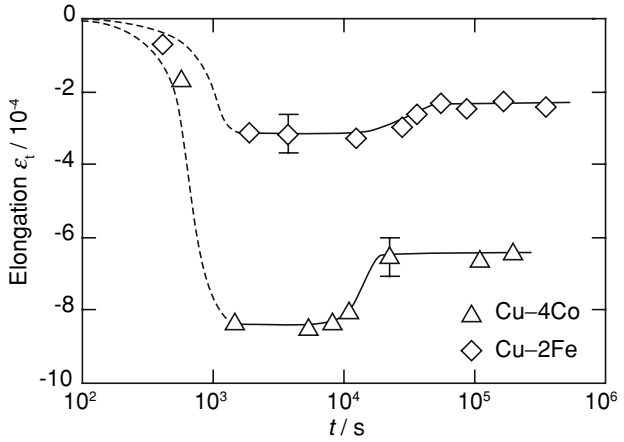

Fig. 8 Variation in the elongations ε_t of Cu–4 wt.%Co and Cu–2 wt.%Fe alloys during aging at 700 °C. Representative error bars are also shown

precipitates, previously mentioned. In addition, the average sizes $r = 8$ and 11 nm of Co and γ-Fe precipitates after aging at 700 °C for 2 and 3 h are coincident with the values of $r_c = 6$ and 10 nm for the transition from the coherent stage to mixed stage. The average sizes $r = 14$ and 20 nm of Co and γ-Fe precipitates after aging at 700 °C for 6 and 15 h are also identical to the values of $r_c = 12$ and 20 nm for the transition from the mixed stage to semi-coherent stage. That is, the first plateau, increase and second plateau stages of ε_t for each alloy correspond to the coherent, mixed, and semi-coherent stages of the precipitation process, respectively.

In contrast to the length-change measurement results of Fig. 8, the lattice constants of the matrix of the Cu–Co and Cu–Fe alloys, determined by usual X-ray analyses showed no essential changes from 0.3614 ± 0.00003 to 0.3614 ± 0.00003 nm and from 0.3615 ± 0.00005 to 0.3615 ± 0.00006 nm during aging at 700 °C and the same as that of Cu, 0.3615 nm. These results are compatible with the results previously obtained that the lattice constants of Cu–Co [24] and Cu–Fe [25] solid solutions exhibit no essential changes with the Co and Fe concentrations up to about 10 wt.% and 80 wt.%. It is evident that the change in specimen dimension is brought about by the change in ε^T of the precipitate. Using values of f obtained from $f = (C_0 - C)/(C_P - C_e)$, where C_0 is the initial concentration of the solute (4.3 at.% for Co and 2.2 at.% for Fe) and C_P is the solute concentration in the precipitate (90 at.% for Co [26] and 100 at.% for γ-Fe), the values of ε^T for the Co and γ-Fe precipitates are estimated from Eq. 5 as -0.020 and -0.015 for the coherent interfaces and -0.015 and -0.012 for the semi-coherent interfaces.

Next, we will estimate values of ε from these values of ε^T. For simplicity, we will introduce the ratio A of the elastic constants of the two phases as a positive dimensionless quantity: $A = C_{p,ijkl}/C_{ijkl}$, where $C_{p,ijkl}$ and C_{ijkl} are the isotropic elastic constants of the precipitate and the matrix, respectively. Then ε^T is written as [27]

$$\varepsilon^T = \frac{3A(1-\nu)\varepsilon}{A(1+\nu)+2(1-2\nu)}, \tag{6}$$

where ν is the Poisson ratio of the Cu matrix. Using the shear modulus of the Cu matrix, $\mu = 75.5$ GPa [28], that of the Co precipitate, $\mu_{\text{fcc Co}} = 129.4$ GPa [29], that of the γ-Fe precipitate, $\mu_{\gamma\text{-Fe}} = 69$ GPa [30], the values of $A = 1.71$ and 0.914 are obtained for the Co and γ-Fe precipitates. Equation 6, using the values of ε^T and A, and $\nu = 0.33$ [31], gives $\varepsilon = -0.018$ and -0.016 for the coherent Co and γ-Fe precipitates, and $\varepsilon = -0.013$ and -0.012 for the semi-coherent Co and γ-Fe precipitates, respectively. The values of ε for the coherent Co and γ-Fe precipitates are in accord with the values of $\varepsilon = -0.019$ and -0.015 calculated using the lattice parameters of the Cu matrix, fcc Co and γ-Fe. Hereafter, ε for the semi-coherent precipitate will be expressed as ε_s.

Figure 9(a) and (b) depicts TEM images of large Co and γ-Fe precipitates after aging at 700 °C for 100 h

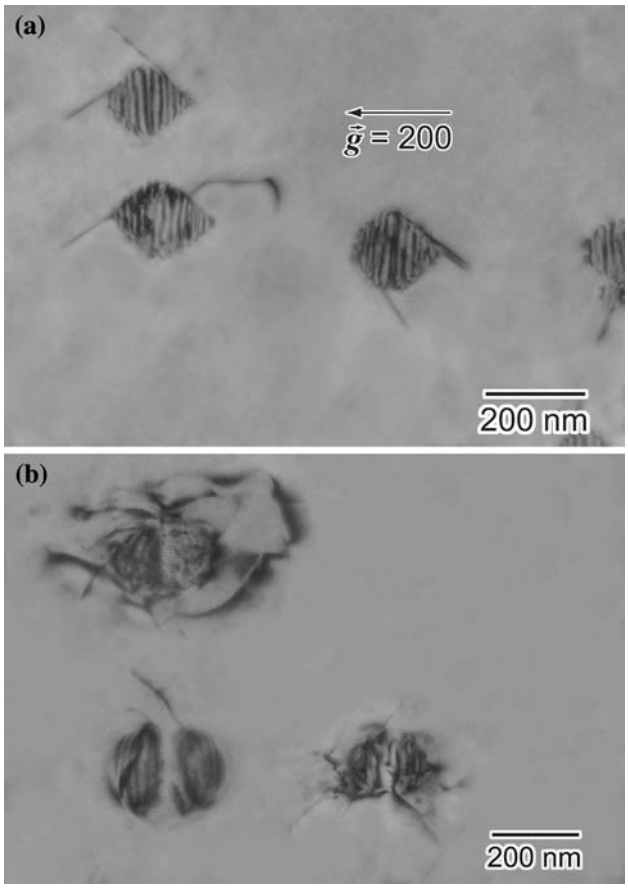

Fig. 9 Bright-field images of (**a**) Co precipitates and (**b**) γ-Fe precipitates in a Cu−4 wt.%Co and a Cu−2 wt.%Fe alloy aged at 700 °C for 100 h. The zone axis is $[011]_{Cu}$

(3.6×10^5 s). Parallel moiré fringes are observed on the Co and γ-Fe precipitates. As shown in Fig. 9(a) and (b), dislocations were generated around Co and γ-Fe precipitates larger than about 25 and 40 nm in radius. The generation of dislocations was noticed around the Co or γ-Fe precipitates initially after aging at 700 °C for about 10 or 40 h (3.6×10^4 or 1.4×10^5 s), and around all the Co or γ-Fe precipitates after aging for about 40 or 50 h (1.4×10^5 or 1.8×10^5 s). It should be noted in Fig. 8 that the elongation of the Cu–Co or Cu–Fe specimen does not change between 10 and 40 h or between 40 and 50 h. Thus, it is concluded that the misfit strains of the Co and γ-Fe precipitates are not released by the generation of dislocations in the matrix but by the formation of the misfit dislocations at the matrix/precipitate interface.

Discussion

The value of $\gamma = 0.15$ J m^{-2} for the Co precipitates derived in this study is identical to the average value of $\gamma = 0.15$ J m^{-2}, previously obtained for the semi-coherent Cu/Co interface [1]. We have also revealed that the experimentally obtained value of $\gamma = 0.15$ J m^{-2} is insensitive to the change in coherency of the Cu/Co interface [1]. On the other hand, the dependence of γ on the interfacial state of Cu/γ-Fe has not yet been investigated, although several investigators [6, 18–21] estimated the value of γ as 0.25 J m^{-2}, which is in good agreement with our value of 0.27 J m^{-2}. Since the values of K for the Cu–Co and Cu–Fe alloys aged at 500 °C in Table 1 were obtained in the coherent stages, as shown in Figs. 4 and 5, it is evident that the values of 0.15 J m^{-2} and 0.27 J m^{-2} are for the coherent Cu/Co and Cu/γ-Fe interfaces. Also the values of K of the Co and γ-Fe precipitates in the present Cu alloys aged at 700 °C exhibit no changes with the transitions of coherency, as shown in Figs. 4 and 6. It is thus stated that the transitions from the coherent Cu/Co and Cu/γ-Fe interfaces to the semi-coherent interfaces do not affect the values of γ, experimentally obtained using the LSW theory. However, it is widely accepted that the formation of misfit dislocations on a coherent interface causes an increase in energy of the coherent interface [7–10]. In the following, this discrepancy will be discussed by examining the driving force for coarsening of the coherent and semi-coherent precipitates.

First, we will estimate the elastic strain energies, E and E_s, per unit volume of the coherent and semi-coherent precipitates. In the case that the coherent spherical precipitates have purely dilatational misfit strains ε, the elastic strain energy E of the spherical precipitate per unit volume is written as [27]

$$E = \frac{6A(1+\nu)}{\{A(1+\nu)+2(1-2\nu)\}}\mu\varepsilon^2. \tag{7}$$

From this equation using the values of A and ν and the experimental values of ε and ε_s, described in the previous section, we have $E = 1.1 \times 10^8$ and 7.0×10^7 J m^{-3} for Co and γ-Fe and $E_s = 5.9 \times 10^7$ and 4.4×10^7 J m^{-3} for Co and γ-Fe, respectively.

The transition from a coherent interface to a semi-coherent interface results in an increase in the interface energy γ [7–10]. The increase in γ occurs by the introduction of misfit dislocations. The increment $\Delta\gamma$ per unit area is expressed as [8]

$$\Delta\gamma = \frac{\mu b}{2\pi^2}\left[1+\beta-(1+\beta^2)^{1/2}-\beta\ln\left\{2\beta(1+\beta^2)^{1/2}-2\beta^2\right\}\right] \tag{8}$$

and

$$\beta = \frac{\pi|\Delta\delta|}{1-\nu}, \tag{9}$$

where $\Delta\delta$ is the change in the interfacial misfit from the coherent interface to the semi-coherent interface. In the present case, $\Delta\delta = |\varepsilon_s - \varepsilon| = 0.0046$ and 0.0032 for Co and γ-Fe, respectively. The values of μ, ν, and b were described in the previous section. Substituting these values into Eqs. 8 and 9, we obtain $\Delta\gamma = 0.086$ J m^{-2} for Co and $\Delta\gamma = 0.065$ J m^{-2} for γ-Fe.

The total free energies, G and G_s, of the coherent and semi-coherent precipitates are given by the equations:

$$G = S\gamma + VE \tag{10}$$

and

$$G_s = S\gamma_s + VE_s, \tag{11}$$

where γ_s is the semi-coherent interface energy of the precipitate and S and V are the interfacial area and volume of the precipitate, respectively. We do not have to consider the chemical potential energy of the two-phase microstructure because the energy does not essentially change with precipitate coarsening when the volume fraction of precipitates does not vary [32]. The driving force ΔG for coarsening of the coherent precipitate can thus be written as [33]

$$\Delta G \equiv \frac{dG}{dn} = \frac{2\gamma V_m}{r} + EV_m. \tag{12}$$

Here, n is the molar concentration of solute atoms ($=4\pi r^3/(3V_m)$). The driving force ΔG_s for coarsening of the semi-coherent precipitate takes a similar form. From Eq. 12 using the values of γ, γ_s, E, and E_s described above, and $r = r_c = 6$ and 10 nm for the Co and γ-Fe precipitates, we obtain $\Delta G = 1.1 \times 10^3$ J mol^{-1} and $\Delta G_s = 9.3 \times 10^2$ J mol^{-1}

for the Co precipitate and $\Delta G = 8.5 \times 10^2$ J mol^{-1} and $\Delta G_s = 7.7 \times 10^2$ J mol^{-1} for the γ-Fe precipitate. For both Co and γ-Fe, the values of ΔG_s are nearly the same as those of ΔG. This corresponds to the fact that the coarsening rates of the Co and γ-Fe precipitates did not change with the transition in precipitate coherency. Therefore, the values of γ and γ_s experimentally derived by the LSW theory can be understood to be seemingly identical, and thus the actual values of γ_s ($=\gamma + \Delta\gamma$) for the semi-coherent Cu/Co interface and Cu/γ-Fe interface can be estimated as about 0.24 and 0.34 J m^{-2}.

When the coherency transition of a precipitate occurs, the sum of the interface and elastic strain energies of the precipitate must be conserved. In other words, the increase in the interface energy, $4\pi r_c^2 \Delta\gamma$, by the introduction of misfit dislocations on a precipitate interface must be equal to the decrease in the elastic strain energy, $4\pi r_c^3 (E - E_s)/3$, by the relaxation of misfit. Usage of the values of r_c, E, and E_s for Co and γ-Fe precipitates described above yields $\Delta\gamma = 0.098$ and 0.086 J m^{-2} for Co and γ-Fe, respectively. Then we have $\gamma_s = 0.25$ and 0.36 J m^{-2} for Co and γ-Fe, respectively. Interestingly, these values are in good agreement with $\gamma_s = 0.24$ and 0.34 J m^{-2} obtained using Eq. 8.

Conclusions

Investigations of the effects of precipitate coherency on the coarsening of Co and γ-Fe precipitates in a Cu–4 wt.%Co and a Cu–2 wt.%Fe alloy aged at 500 and 700 °C by means of transmission electron microscopy (TEM) observations, electrical resistivity measurements, and length-change measurements have yielded the following conclusions:

(1) The shape of γ-Fe precipitates changes from a sphere to a cube faceted on $\{001\}_{Cu}$ planes at a radius of about 25 nm.
(2) The radii at which the transitions occur from the coherent Cu/Co and Cu/γ-Fe interfaces to the semi-coherent interfaces are determined as 6–12 nm and 10–20 nm from TEM image analyses.
(3) The transition in precipitate coherency causes no changes in the coarsening rates of Co and γ-Fe precipitates in the Cu matrix.
(4) Analyses of length-change measurement results reveal that the isotropic misfit strains of the Co and γ-Fe precipitates are -0.018 and -0.016 for the coherent interfaces, and -0.013 and -0.012 for the semi-coherent interfaces, respectively.
(5) The coherent Cu/Co and Cu/γ-Fe interface energies are obtained as 0.15 and 0.27 J m^{-2} by application of the LSW theory. Free energy analyses show that the semi-coherent Cu/Co and Cu/γ-Fe interface energies are 0.24 and 0.34 J m^{-2}.

Acknowledgements We thank Professor K. Tazaki, Kanazawa University, for use of JEOL2010FEF. We also acknowledge Mr. K. Higashimine of the Center for Nano Materials and Technology, Japan Advanced Institute of Science and Technology, for the TEM observation by HITACHI H9000-NAR.

References

1. Watanabe D, Higashi K, Watanabe C, Monzen R (2007) J Jpn Inst Metals 71:151
2. Lifshitz IM, Slyozov VV (1961) J Phys Chem Solids 19:35
3. Wagner C (1961) Z Elektrochem 65:581
4. Ardell AJ (1967) Acta Metall 15:1772
5. Easterling KE, Miekk-Oja HM (1967) Acta Metall 15:1133
6. Monzen R, Kita K (2002) Philos Mag Lett 82:373
7. Iwamura S, Miura Y (2004) Acta Mater 52:591
8. Jesser WA (1969) Philos Mag 19:993
9. Røyset J, Ryum N (2005) Scripta Mater 52:1275
10. Fuller CB, Seidman DN (2005) Acta Mater 53:5415
11. Johnson WC (1984) Acta Metall 32:465
12. Ashby MF, Brown LM (1963) Philos Mag 8:1083
13. Ashby MF, Brown LM (1963) Philos Mag 8:1649
14. Linde JO (1968) Helv Phys Acta 41:1007
15. Heinrich B, Cochran JF, Kowalewski M, Kirschner J, Celinski Z, Arrott AS, Myrtle K (1991) Phys Rev B 44:9348
16. Kato M, Monzen R, Mori T (1978) Acta Metall 26:605
17. Kinzoku data book (2004) Japan Institute of Metals, Maruzen, Tokyo, p 37
18. Matsuura K, Kitamura M, Watanabe K (1977) J Jpn Inst Metals 41:1285
19. Fujii T, Kato M, Mori T (1991) Mater Trans Jpn Inst Metals 32:229
20. Watanabe Y, Kato M, Sato A (1991) J Mater Sci 26:4307
21. Ezawa T (1988) Z Metallkd 9:572
22. Eshelby JD (1959) Proc R Soc A 252:561
23. Monzen R, Watanabe C, Seo T, Sakai T (2005) Philos Mag Lett 85:603
24. Gente C, Oehring M, Bormann R (1993) Phys Rev B 48:13244
25. Chien CL, Liou SH, Kofalt D, Yu W, Egami T, McGuire TR (1986) Phys Rev B 33:3247
26. Wendt H, Haasen P (1985) Scripta Metall 19:1053
27. Kato M, Fujii T, Onaka S (1996) Mater Sci Eng A 211:95
28. Rayne JA (1958) Phys Rev 112:1125
29. Satoh S, Johnson WC (1992) Metall Trans A 23:2761
30. Pope LE, Rohde RW, Percival CM (1976) Metall Trans A 7:103
31. Shindohin data book (1997) Japan Copper and Brass Association, Tokyo, p 42
32. Miyazaki T, Koyama T (1993) Mater Sci Eng A 169:159
33. Ryu HJ, Hong SH, Weber J, Tundermann JH (1999) J Mater Sci 34:329